Supplementary Information

Active mechanics and dynamics of cell spreading on elastic substrates

Noam Nisenholz, Kavitha Rajendran, Quynh Dang, Hao Chen, Ralf Kemkemer, Ramaswamy Krishnan, and Assaf Zemel

I. ANALYSIS OF SLIP-BOND AND CATCH-BOND MECHANISMS OF NON-LINEAR CELL-SUBSTRATE FRICTION

The density of engaged adhesion sites, N_b, and the mean displacement, $\langle s \rangle$, are in general functions of the sliding speed, v_F, the density of ligands on the surface, N_L, and the binding/unbinding kinetic rates of ligands to the cytoskeleton. To predict these dependencies we exploit a simple stochastic model for the binding kinetics at the cell-matrix interface, inspired by Walcott et al. [1]. We denote by $n(s,t)$ the number of engaged actin-ECM adhesions present in a unit area of the the adhesion layer with displacement between s and $s+ds$ at time t. The rate of change in $n(s,t)$ is given by :

$$\frac{\partial n(s,t)}{\partial t} = -v_F \frac{\partial n(s,t)}{\partial s} + k_b\, g(s)\, N_{ub}(t)\, N_L - k_{ub}(s)\, n(s,t) \tag{S1}$$

with the normalization condition given by $\int_{-\infty}^{\infty} n(s,t)ds = N_b(t)$ and $N_{ub}(t) = N - N_b(t)$. Here, $k_b\, N_L$ and $k_{ub}(s)$ are the binding/unbinding pseudo-first-order rate constants, respectively. The function $g(s)$ accounts for the probability that a connection will form with non-vanishing displacement, s. While thermal energy and other stochastic mechanisms are likely to broaden $g(s)$, in the following we shall adopt the simplest assumption possible, that $g(s)$ is a delta function $\delta(s)$, namely, that connections always form with zero displacement (for a more general treatment, see e.g., [2]).

Eq. S1 provides a master equation for the density distribution, $n(s,t)$, of actin-ECM bonds existing with displacement s at time t. Under the assumption that new bonds always form with zero displacement, $g(s) = \delta(s)$, one finds the following solution for $n(s)$ at steady state:

$$n(s) = \frac{N \exp\left[\frac{-1}{v_F}\int_0^s k_{ub}(s')ds'\right]\theta(s)}{\frac{v_F}{k_b} + \int_0^\infty \exp\left[\frac{-1}{v_F}\int_0^s k_{ub}(s')ds'\right] ds} \tag{S2}$$

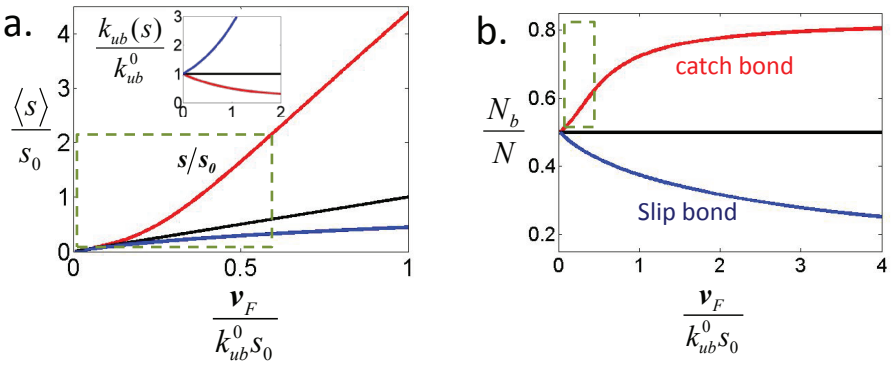

FIG. S1. (a.) Normalized mean bond displacement, $\langle s\rangle/s_0$, and (b.) density of bound integrins, N_b/N, as function the retrograde flow speed, for three choices of the unbinding rate functions (shown in the inset): in blue, a slip-bond behavior is examined, $k_{ub}(s) = k^0_{ub}\, e^{s/s_0}$, in red, $k_{ub}(s) = k^1_{ub} + (k^0_{ub} - k^1_{ub})\, e^{-s/s_0}$, a catch bond behavior is shown, and black is for the fixed unbinding rate, $k_{ub} = k^0_{ub}$. Parameters used in this calculation, $k_b = k^0_{ub} = 1.0\,\mathrm{sec}^{-1}$, $k^1_{ub} = 0.2\,\mathrm{sec}^{-1}$, and $s_0 = 0.05\,\mu m$. The value of v_{pol} dictates the regime in the graphs (green box) where the spreading dynamics occurs because spreading ends ($v = 0$) when $v_F = v_{pol}$. The concave shape of $\langle s\rangle$ in the catch bond case (red curve) is consistent with the experimental form of the force-velocity relation. To see this recall that $f \sim N_b\langle s\rangle$ and that the abscissa shown here, $v_F = v_{pol} - v$, should be inverted to plot $f(v)$ (see Fig. 4 in main text). To obtain the concave behavior of $\langle s\rangle$ within a regime that is sampled during spreading, a relatively large ratio s_0/v_{pol} is needed; as a compromise we chose $v_{pol} = 1.8\,\mu m/\mathrm{min}$ and $s_0 = 0.05\,\mu m$ which is generally larger than one might expect.

where $\theta(s)$ is the Heaviside step function. This solution can be integrated to find the the mean displacement, $\langle s\rangle$, and density of bound integrin connections, N_b, via:

$$\langle s\rangle = \frac{1}{N_b}\int_0^\infty s\, n(s) ds \quad \text{and} \quad N_b = \int_0^\infty n(s) d\, s \tag{S3}$$

This generalizes the simpler result, $\langle s\rangle = v_F/k^0_{ub}$, and $N_b/N = N_L/(N_L + k^0_{ub}/k_b)$ obtained previously (Eq. 2) for the displacement-independent unbinding rate case $k_{ub}(s) = k^0_{ub}$.

Motivated by experiments (see text) we studied the following two contrasting functional forms of $k_{ub}(s)$: (i) a slip-bond dependence (Bell's mechanism), $k_{ub}(s) = k^0_{ub}\, e^{s/s_0}$ and, (ii) a catch-bond dependence, $k_{ub}(s) = k^1_{ub} + (k^0_{ub} - k^1_{ub})\, e^{-s/s_0}$, where k^0_{ub}, k^1_{ub} and s_0 are constants; these were compared to the previously studied case, $k_{ub}(s) = k^0_{ub}$.

The integrals appearing in Eqs. S2, S3, and the one used to calculate N_b have been calculated numerically and the results are summarized in Fig. S1; analytical solutions for both these cases

can be found in terms of hypergeometric functions (e.g., see [3]). Panels a. and b. of Fig.S1, respectively show the variations of $\langle s \rangle$ and N_b with the (normalized) pulling velocity, v_F. Blue curves correspond to the slip-bond dependence, red curves to the catch-bond dependence, and the black lines for the constant unbinding rate case. As expected for a slip-bond mechanism (blue curves), adhesion contacts destabilize with higher pulling velocities (v_F) hence the total number of bound anchors, N_b, decreases. The opposite behavior is exhibited for the catch bond case; the total number of bonds, N_b, increases with v_F, up to the saturating value $N_b = N\frac{k_b}{k_b+k_{ub}^1}$. For these high v_F values, the displacement s can be so large (relative to s_0) that $k_{ub}(s) = k_{ub}^1 + (k_{ub}^0 - k_{ub}^1)\, e^{-s/s_0} \to k_{ub}^1$ and hence N_b obtains a similar expression as in the linear theory but with the replacement of k_{ub}^0 by k_{ub}^1. The average displacement $\langle s \rangle$ shows a somewhat more complicated behavior. In both mechanisms there is a steady increase of $\langle s \rangle$ with v_F for low values of v_F; the increase is more significant in the catch bond case since bonds that stay connected further get pulled when the velocity is higher. The increase of N_b with v_F thus feeds back on $\langle s \rangle$ and causes its dramatic increase. This influence of N_b on the dependence of $\langle s \rangle$ on v_F ends when N_b reaches its saturation value. At this point $\langle s \rangle$ continues to grow linearly with v_F but with the slope $1/k_{ub}^1$, namely as, $\langle s \rangle \sim v_f/k_{ub}^1$. Hence a second *linear*, force-velocity-relation is reached at high sliding velocities. In the slip-bond mechanism case, the gradual decrease of N_b with v_F competes with the general tendency of s to grow with v_F, hence the outcome is a well known non-monotonic dependence of $f \sim N_b \langle s \rangle$ on v_F with a maximum for some intermediate value (not shown here but see [4]). We note that the figure displays the behavior for velocities that can be much larger than those that can be reached physiologically since spreading ceases when $v_F = v_{pol}$, and hence v_{pol} places a limit on the possible range of v_F. The green box in this figure shows a reasonable range of the normalized velocity v_F with appropriate choice of parameters.

Expanding the product $N_b \langle s \rangle$ to second order in powers of $v_F = v_{pol} - v$ we obtain the following expression for $f = L_l N_b \kappa \langle s \rangle$:

$$\frac{f_\pm}{\xi_s v_{pol}} = \left(1 - \frac{v}{v_{pol}}\right) \pm C \frac{v_{pol}}{s_0 k_{ub}^0} \left(1 - \frac{k_{ub}^1}{k_{ub}^0}\right) \left(1 - \frac{v}{v_{pol}}\right)^2 \tag{S4}$$

where the $(+)$ and $(-)$ expressions are for the catch-bond and slip-bond mechanisms, respectively; the slip-bond mechanism also implies $k_{ub}^1 = 0$. We also defined $C = \frac{(5-2\beta)}{(2-\beta)}$, with $\beta = \frac{k_b}{k_b+k_{ub}^0}$, and maintained the previous definition of $\xi_s = L_l N_b \kappa / k_{ub}^0$. These expansions generalize the linear force-velocity relation obtained previously in Eq. 5. However, while in the linear theory $\xi_s v_{pol}$ represented the stall force f_{ss}, this isn't so in the case at hand. Rather, the stall force is obtained

when $v = v_{pol} - v_F = 0$, or when, $v_F = v_{pol}$. This force can be extracted from our numerical plots by choosing a point on the x-axis such that $v_F = v_{pol}$, as illustrated with the green box in Fig. S1. One may also calculate an approximate stall force from the expansion in Eq. S4, however, our numerical calculations show that this (primarily in the catch-bond case) significantly underestimates the marked effect that k_{ub}^1 and s_0 have on the stall force. The expansion of Eq. S4 is useful, however, for gaining intuition for how the various parameters affect the force-velocity relation. Thus, as expected, the smaller s_0 the stronger the non-linear effect. For the catch-bond case, lower k_{ub}^1 or s_0 results in *larger* forces. In contrast, for the slip-bond mechanism, *smaller* forces are expected for smaller values of s_0.

To predict the dynamics observed in Fig. 4, Eq.S3 is combined with Eqs.2 and 3, and solved numerically, since the force velocity relation predicted analytically by Eq.S3 is a highly complex function of v.

---

[1] Walcott, S. & Sun, S. A mechanical model of actin stress fiber formation and substrate elasticity sensing in adherent cells. *Proc. Natl. Acad. Sci.* **107**, 7757 (2010).

[2] Vilfan, A., Frey, E. & Schwabl, F. Force-velocity relations of a two-state crossbridge model for molecular motors. *EPL (Europhysics Letters)* **45**, 283 (1999).

[3] Srinivasan, M. & Walcott, S. Binding site models of friction due to the formation and rupture of bonds: state-function formalism, force-velocity relations, response to slip velocity transients, and slip stability. *Physical Review E* **80**, 046124 (2009).

[4] Harland, B., Walcott, S. & Sun, S. X. Adhesion dynamics and durotaxis in migrating cells. *Physical biology* **8**, 015011 (2011).